Arabian Journal of Geosciences (2019) 12: 490
https://doi.org/10.1007/s12517-019-4638-z

TECHNICAL NOTE

Changing temporal and spatial patterns of fluvial sedimentation in Three Gorges Reservoir, Yangtze River, China

Yi Xiao[1] · Wenjie Li[1] · Shengfa Yang[1]

Received: 30 October 2018 / Accepted: 10 July 2019 / Published online: 1 August 2019

Abstract

The impoundment of the Three Gorges Reservoir (TGR) alters the hydrodynamic conditions and sediment movements related to fluvial sedimentation in the upper stream of the Yangtze River. Based on an extensive dataset of the daily discharge, sediment transport rate, and riverbed level collected from 2003 to 2016 in the TGR area, we applied a Mann–Kendall test, the rescaled range (R/S) analysis method, and 2D numerical modeling to investigate the controls of the temporal–spatial reservoir sedimentation process and their changing trends. The results indicate that (1) the decreasing trends of annual runoff in the upstream of the Yangtze River and its main tributaries are insignificant, and a rapid decrease is not likely to occur, (2) the turning points of the temporal variations in the annual runoff–sediment discharge of the TGR were in 1991 and 2002, (3) the response of the channel pattern to the reservoir sedimentation can be a main factor in controlling the spatial distribution of sedimentation, and (4) an adjustment of the reservoir pool-level can directly influence the sediment processing in the TGR. In the future, dam constructions on the main stem of the Yangtze River and its major tributaries will further decrease the sediment discharge and alleviate sedimentation in the TGR.

Keywords Fluvial sedimentation · Runoff–sediment discharge · Channel pattern · The Three Gorges Reservoir · Yangtze River

Introduction

Fluvial sedimentation occurs primarily in response to interactions among natural factors such as the surface material, precipitation, river runoff, sediment supply, and topography. As populations increase, however, reservoir construction, sand excavation, bank revetments, and land use alterations significantly change the natural dynamics of the river channels (Wang et al. 2012). Anthropogenic impacts on the channel morphology and fluvial processes are also becoming increasingly important factors, particularly dam construction and water diversion for water and energy needs (Nilsson et al. 2005). Dams can disrupt the river continuity, intercept the sediment, and change the fluvial hydrology, leading to altered channel patterns (Graf 2006, Kiss et al. 2008; Lu and Jiang 2009; Yang et al. 2010; Marwan et al. 2011).

More than 45,000 dams have been constructed on major rivers worldwide, and significant progress has been made in the study of downstream river dynamics in response to the changes in climate, river runoff, and sediment transport (Aleem 1972; Batalla et al. 2004; Kummu et al. 2010; Draut et al. 2011). The Three Gorges Reservoir (TGR) is located in the middle stretch of China's largest river, the Yangtze River, and as the world's largest hydropower project, the Three Gorges Project is a key to harnessing and exploiting the power of the river (Fig. 1). The construction of the TGR has altered the hydrodynamic conditions and sediment movements in the upstream areas of the Yangtze River, leading to a dramatic decrease in sediment fluxes in the middle and lower reaches. Recent research has focused on the changing trends of water–sediment discharge and channel patterns downstream (Xiong et al. 2009; Li et al. 2011; Yang et al. 2011; Dai and Lu 2014; Gao et al. 2015), as well as the material fluxes and water exchanges between the Yangtze River and large lakes (Yang et al. 2011; Guo

Editorial handling: Ozgur Kisi

✉ Yi Xiao
xymttlove@163.com

[1] National Inland Waterway Regulation Engineering Research Center, Chongqing Jiaotong University, Chongqing, China

Fig. 1 Backwater region of the Three Gorges Reservoir

et al. 2012; Sun et al. 2012; Dai and Liu 2013; Cheng et al. 2018).

The backwater area of the TGR is approximately 660 km long, stretching from Yichang to Chongqing (Fig. 1). After the pool level of the TGR was increased to 175 m in 2008, the 432-km-long permanent backwater zone stretched from the dam to Fuling, and the fluctuating backwater region extended to Jiangjin (Fig. 2). The TGR became fully operational in 2009 and has the largest storage capacity (39.3 billion cubic meters (bcm)) in the Yangtze River basin, constituting approximately 4.5% of the Yangtze's annual discharge. Studies on the backwater area of the TGR have focused on environmental and landslip impacts (Yan et al. 2008; Zhang et al. 2009; Wolf et al. 2013; Zhou et al. 2016), and few investigations have examined the control on the temporal–spatial distribution of the sedimentation process or quantified the sections with the main deposition reach in the backwater region, although sedimentation is a key to the navigation conditions and is closely related to the environment and fish habitats in the reservoir area.

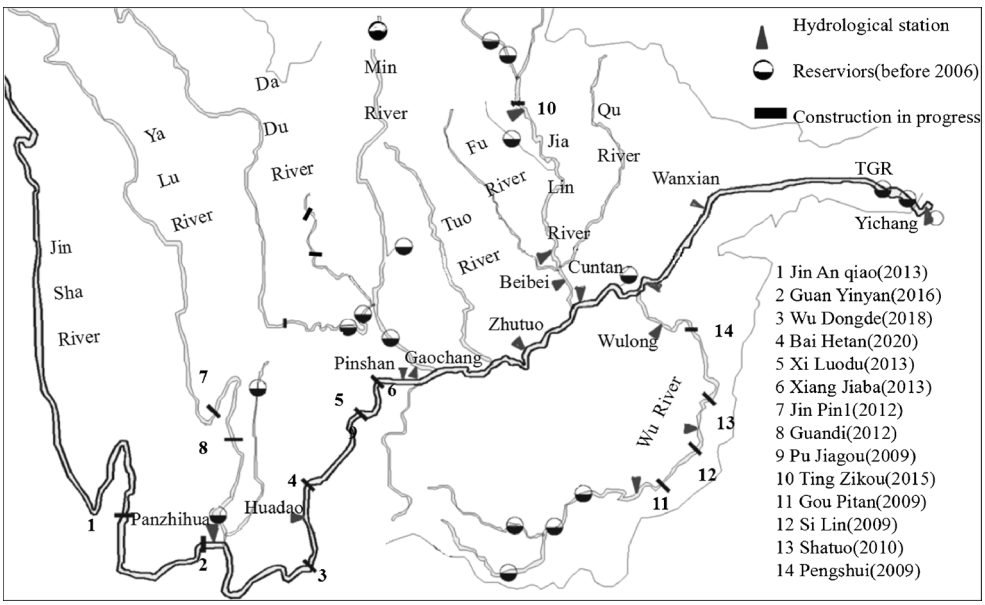

Fig. 2 Distribution of the main hydrological stations

The Mann–Kendall (M–K) test and rescaled range (R/S) analysis method were applied to detect the temporal–spatial distributions of the variations in annual runoff–sediment transport and their changing trends. The combination of a newly developed two-dimensional (2D) numerical model with field measurements at a typical reach in the TGR was applied to analyze the relation between the river pattern and the distribution of the reservoir sedimentation. Our objectives were to (1) analyze the variations in the annual runoff–sediment transport to discuss the controls on the spatial–temporal sedimentation process; (2) reveal the spatial distribution of the reservoir sedimentation over the past decade, focusing particularly on the main depositional reaches in the permanent backwater area; and (3) evaluate the change trends of the sedimentation pattern in the TGR.

Materials and methods

Gaochang station is the control point for the main tributary of the Min River joining the upper Yangtze River, Zhutuo station is located above the Chongqing reach section, Beibei station is the control for the Jialing River that joins the Yangtze River, and Cuntan station is the inflow control point of the upper Yangtze River into the TGR (Fig. 2). This study is based on an extensive dataset of daily water discharge from 1954 to 2016, the sediment transport rate, the riverbed level collected from the four control hydraulic stations above (Sediment-Panel 2016), and the 2003–2013 field measurements of the streambed topography in the TGR area.

Mann–Kendall test

The temporal–spatial distributions of the runoff and sediment discharge were based on the sequential Mann–Kendal test applied to nonparametric statistics. This test has typically been used in the fields of hydrology and climatology to test the degree of randomness against the trend from the hydrologic time-series (Sneyers 1990; Yue et al. 2002). As a rank-based procedure, this test is robust to the influence of extremes and its application is good for skewed data. The measurements (observations or data) obtained over time must be independent and identically distributed. With this method, a rank S_k is established for the time-series using a sample space:

$$S_k = \sum_{i=2}^{k} \sum_{j=1}^{i} r_j (k = 2, 3, \ldots, n) \tag{1}$$

when $1 \le j \le i$, $x_i > x_j$, $1 \le j \le i$, $r_i = 1$, or $r_i = 0$.

Based on the assumption that the time-series was independent, we defined the following:

$$UF_k = \frac{(S_k - E(S_k))}{\sqrt{Var(S_k)}} (k = 2, 3, \mathrm{K}, n) \tag{2}$$

where $\mathrm{UF}_1 = 0$, and $E(S_\mathrm{k})$ and $Var(S_k)$ are the average value and variance of the accumulated value $\mathrm{S_k}$ when x_1, x_2, $\Lambda\, x_n$ are independent and have the same continuous distribution. The terms $E(S_\mathrm{k})$ and $Var(S_k)$ can be expressed as follows:

$$E(S_\mathrm{k}) = \frac{n(n-1)}{4} \quad Var(S_\mathrm{k}) = \frac{n(n-1)(2n+5)}{72} \tag{3}$$

where $\mathrm{UF_i}$ is the standard normal distribution based on the statistics of the time-series x_1, x_2, $\Lambda\, x_n$. According to the significance level α, if $|UF_i| > U_{a/2}$, the change trend of the time-series is clear. Thus, according to the reverse order of the time-series x_n, x_{n-1}, $\Lambda\, x_1$, the above process is repeated, and $\mathrm{UB_k} = -\mathrm{UF_k}$, $k = n$, $n-1$, K, 1, and $\mathrm{UB}_1 = 0$. From the $\mathrm{UF_k}$ and $\mathrm{UB_k}$ characteristic curves, if $\mathrm{UF_k}$ or $\mathrm{UB_k} > 0$, a monotonic upward trend indicates that the variable consistently increases over time, although the trend may or may not be linear; in addition, a value of < 0 indicates that a decreasing trend occurs over time. Values that exceed the critical curve imply a clear changing trend. A catastrophic change may occur if the value of $\mathrm{UF_k}$ or $\mathrm{UB_k}$ exceeds the significance level, namely, $\alpha = 0.01$. Characteristic curves between the critical curves signal a rapid change in the time-series.

R/S analysis method

The trend changes of the runoff and sediment transport were based on the R/S analysis, distinguished by the value of Hurst index H ($0 < \mathrm{H} < 1$). For the time-series $k(t)$, $t = 1$, 2, Λ, for any natural number $j \ge t \ge 1$, we defined the index as follows:

$$\text{average value,} \quad k_j = \frac{1}{j} \sum_{t=1}^{j} k(t); \tag{4}$$

$$\text{cumulative deviation,} \quad X(t,j) = \sum_{u=1}^{j} \left(k(u) - k_j\right); \tag{5}$$

$$\text{range,} \quad R(j) = \max X(t,j) - \min X(t,j); \tag{6}$$

$$\text{standard deviation,} \quad S(j) = \left[\frac{1}{j} \sum_{t=1}^{j} \left(k(t) - k_j\right)^2\right]^{1/2} \tag{7}$$

Table 1 Mean annual runoff and sediment discharge in the upper Yangtze River

River basin		Min river	Yangtze River	Jialing River	Yangtze River
Control station		Gaochang	Zhutuo	Beibei	Cuntan
Mean annual runoff ($10^8 m^3$)	Before 1990	882	2659	704	3520
	1991–2002	815	2672	529	3339
	Variation ratio	− 8%	1%	− 25%	− 5%
	2003–2012	789	2524	660	3279
	Variation ratio	− 11%	− 5%	− 6%	− 7%
	Annual average	843	2631	658	3440
Mean annual sediment load ($10^4 t$)	Before 1990	5260	31,600	13,400	46,100
	1991–2002	3450	29,300	3720	33,700
	Variation ratio	− 34%	− 7%	− 72%	− 27%
	2003–2012	2930	16,800	2920	18,700
	Variation ratio	− 44%	− 47%	− 78%	− 59%
	Annual average	4400	27,800	10,000	38,500

The term (lnj,lnR/S) is fitted using the method of least squares, and the slope of the straight line is the Hurst index H. The process of the time-series is independent and random when $H = 0.5$; $H < 0.5$ indicates that the changing trend is opposite from the previous state, and $H > 0.5$ indicates the maintenance of the previous condition.

2D hydrodynamic numerical model

The hydrodynamic portion of the 2D numerical model and its verification were fully described by Xiao et al. (2012), who solved the Reynolds-averaged Navier–Stokes equations of mass and momentum conservation in an orthogonal curvilinear grid system:

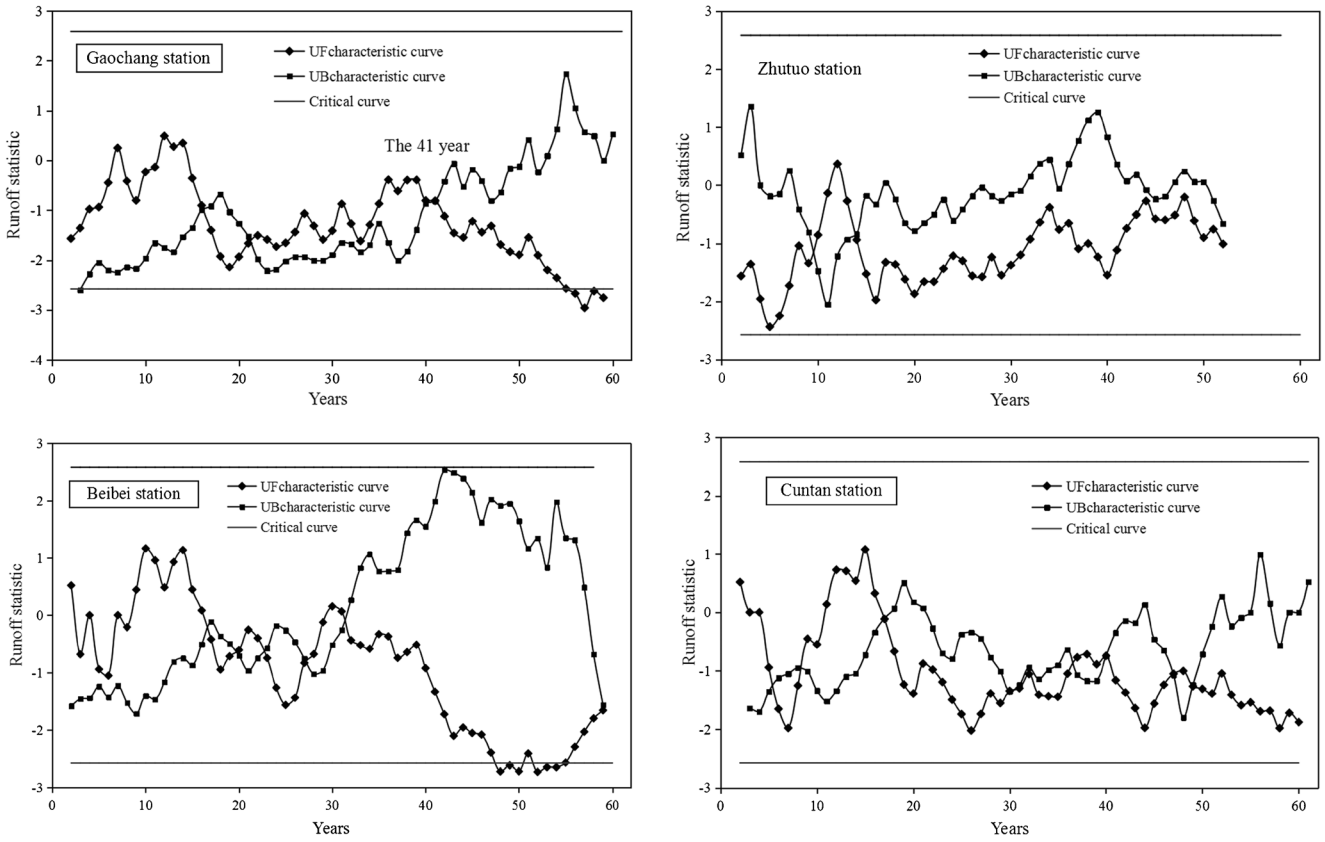

Fig. 3 UF–UB curve of the mean annual runoff at the main control stations

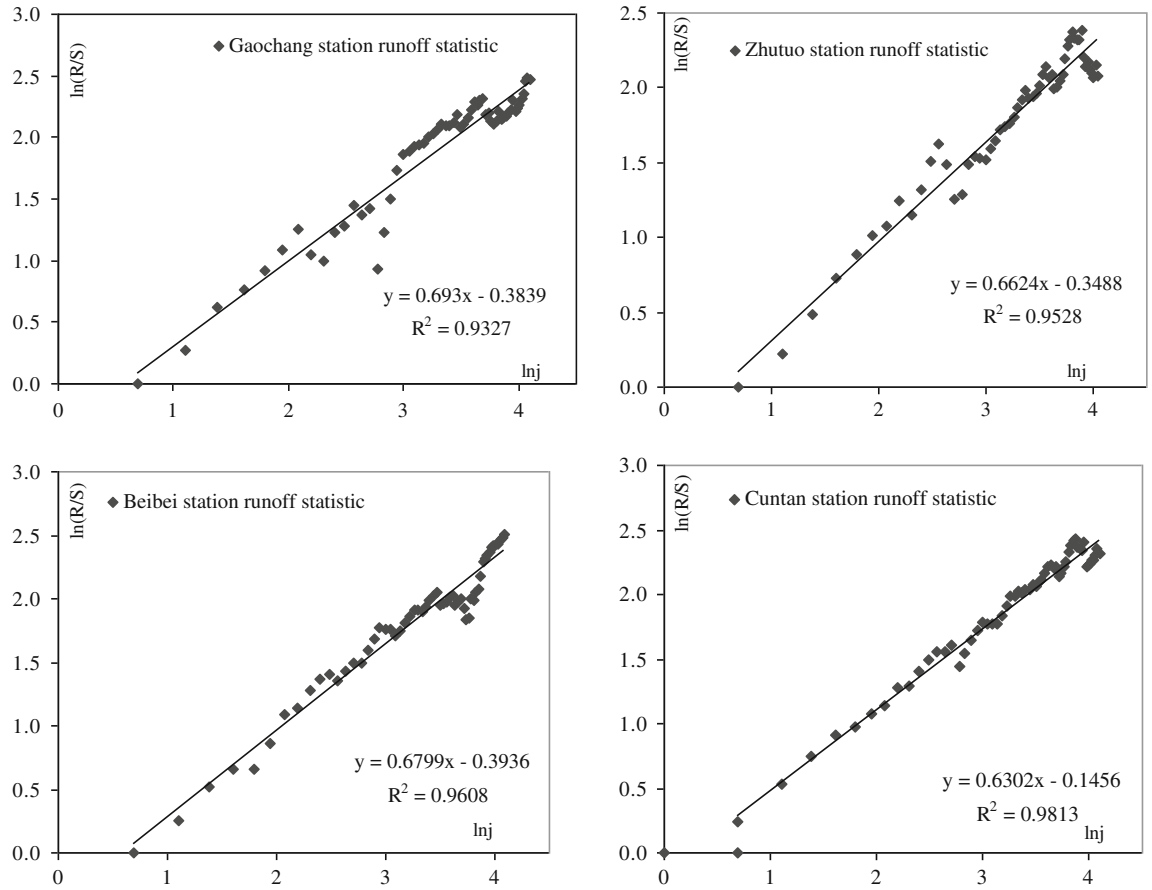

Fig. 4 R/S trend curve of the annual runoff for the control stations

$$\frac{\partial Z}{\partial t}+\frac{1}{J}\left[\frac{\partial(h_2 q)}{\partial \xi}+\frac{\partial(h_1 p)}{\partial \eta}\right]=0$$

$$\frac{\partial q}{\partial t}+\beta\left(\frac{1}{J}\frac{\partial(h_2 qU)}{\partial \xi}+\frac{1}{J}\frac{\partial(h_1 pU)}{\partial \eta}-\frac{pV}{J}\frac{\partial h_2}{\partial \xi}+\frac{qV}{J}\frac{\partial h_1}{\partial \eta}\right)-fp+\frac{gH}{h_1}\frac{\partial Z}{\partial \xi}+\frac{qg|\overline{q}|}{(CH)^2}$$
$$=\frac{\upsilon_e H}{h_1}\frac{\partial E}{\partial \xi}-\frac{\upsilon_e H}{h_1}\frac{\partial F}{\partial \eta}+\frac{1}{J}\frac{\partial(h_2 D_{11})}{\partial \xi}+\frac{1}{J}\frac{\partial(h_{11} D_{12})}{\partial \eta}+\frac{1}{J}\frac{\partial h_1}{\partial \xi}D_{12}-\frac{1}{J}\frac{\partial h_2}{\partial \xi}D_{22}$$

$$\frac{\partial p}{\partial t}+\beta\left(\frac{1}{J}\frac{\partial(h_2 qV)}{\partial \xi}+\frac{1}{J}\frac{\partial(h_1 pV)}{\partial \eta}+\frac{pU}{J}\frac{\partial h_2}{\partial \xi}-\frac{qU}{J}\frac{\partial h_1}{\partial \eta}\right)+fp+\frac{gH}{h_2}\frac{\partial Z}{\partial \eta}+\frac{pg|\overline{q}|}{(CH)^2}$$
$$=\frac{\upsilon_e H}{h_2}\frac{\partial E}{\partial \eta}+\frac{\upsilon_e H}{h_1}\frac{\partial F}{\partial \xi}+\frac{1}{J}\frac{\partial(h_2 D_{12})}{\partial \xi}+\frac{1}{J}\frac{\partial(h_1 D_{22})}{\partial \eta}-\frac{1}{J}\frac{\partial h_1}{\partial \eta}D_{11}+\frac{1}{J}\frac{\partial h_2}{\partial \xi}D_{12}$$

$$E=\frac{1}{J}\left[\frac{\partial(h_2 U)}{\partial \xi}+\frac{\partial(h_1 V)}{\partial \eta}\right],\ F=\frac{1}{J}\left[\frac{\partial(h_2 V)}{\partial \xi}-\frac{\partial(h_1 U)}{\partial \eta}\right]$$

$$h_1=\sqrt{\left(\frac{\partial x}{\partial \xi}\right)^2+\left(\frac{\partial y}{\partial \xi}\right)^2},\ h_2=\sqrt{\left(\frac{\partial x}{\partial \eta}\right)^2+\left(\frac{\partial y}{\partial \eta}\right)^2} \tag{8}$$

where ξ and η are the orthogonal curvilinear coordinates; h_1 and h_2 are the Lamé coefficients; J is the Jacobian of the transformation, $J=h_1h_2$; U and V are the depth-averaged velocity components in the ξ and η directions, respectively; the unit discharge vector is $\overline{q}=(q,p)=(UH,VH)$; Z is the water level relative to the reference plane; H is the total water depth; β is the correction factor for the non-uniformity of the vertical velocity; f is the Coriolis parameter; g is the gravitational acceleration; C is the Chezy coefficient; υ_e is the mean effective vortex viscosity at a particular depth; and D_{11}, D_{12}, D_{21}, and D_{22} are the depth-averaged dispersion stress terms. The effect of the secondary currents is considered using the method by Lien et al. (1999):

$$D_{11}=-\int_{z_b}^{z_s}(u-U)^2dz, D_{22}=-\int_{z_b}^{z_s}(v-V)^2dz, D_{22}=D_{21}$$
$$=-\int_{z_b}^{z_s}(u-U)(v-V)^2dz \tag{9}$$

where u and v are time-averaged velocity components, and z_s and z_b are the dependent water levels of the water surface and channel bed, respectively.

The numerical solution of this model is based on a finite difference method in an orthogonal curvilinear coordinate system. The finite difference equations corresponding to the differential equations are expressed in an implicit form with an alternating direction. All discretization procedures are based on a second-order central difference scheme, except for the time differentials of the water level in a continuity equation, which uses a forward difference scheme. For the advective accelerations in the momentum equations, a combination of the first-order upwind scheme and second-order central difference can be used.

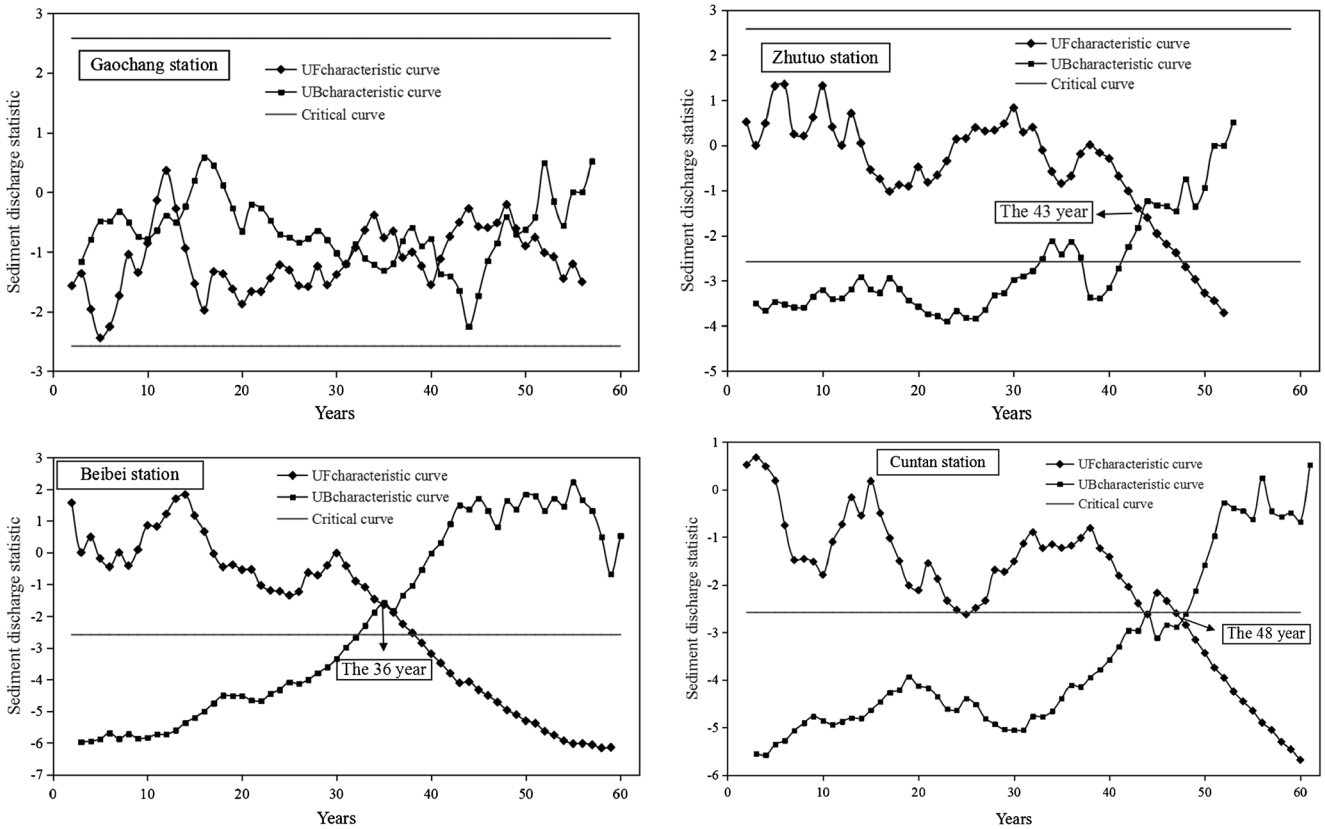

Fig. 5 UF–UB curve of the mean annual sediment discharge at the control stations

Results and discussion

Temporal variations in runoff–sediment load relationship

The patterns of variation in the decade-averaged runoff over the past 30 years (Table 1) at the four hydrological stations show that the average runoff during the first 10 years of operation from 2003 to 2012 is similar to the long-term runoff over the past 20 years (CWRC 2013). Compared with the pre-1990 levels, the control points for the major tributaries of the Yangtze River (Min River, Jialing River) decreased slightly by 6–11%, accounting for the 7% decrease at Cuntan station. By comparing the dataset from 2003 to 2012 with that from 1991 to 2002, the average runoff of the Min and Jialing rivers shows decreasing and increasing trends of approximately 3% and 19%, respectively. The mean sediment load of the time-series for each 10-year period over the past 30 years (1980–2012) from the control hydrological stations (Table 1) shows an overall decrease in sediment load at all of the major stations in comparison with the time-series before the 1990s.

The main tributaries of the Yangtze River have experienced a rapid decrease in sediment load, contributing to a sharp decline in the sediment load at Cuntan station. For example, the annual runoff at the Zhutuo and Beibei stations for 2003–2012 was 2524 and 660 × 108 m^3, respectively, and the annual suspended sediment load decreased by approximately 47% (0.168×10^9 t) and 78% (0.029×10^9 t), respectively, compared with the time-series before the 1990s. Considering that the average value cannot reveal the changing trends of the runoff–sediment discharge and the turning points, we used the characteristic curves of the M–K test and the R/S analysis method to investigate the temporal distribution and changing trends of the variations in the annual runoff–sediment transport.

The UF–UB curve of the mean annual runoff from 1954 to 2016 at the control stations of Gaochang, Zhutuo, Beibei, and Cuntan (Fig. 3) shows the control points for the upstream Yangtze River and its main tributary rivers. The UF values are typically < 0, and the range of fluctuation was between the critical lines except at Gaochang and Beibei stations, indicating a slight decreasing trend in the annual runoff in the Min and Yangtze rivers. The value of the UF curve at Beibei station exceeded the critical line in 1988; the annual runoff declined in the following 10 years (1989–2001) and then began to return to the significance level of the 2002 regime. This pattern revealed a clear increasing trend from 2009 to 2016. The changing trends of the annual runoff for the control stations are indicated by H > 0.5. The values were 0.69, 0.66, 0.68, and 0.64, respectively, during those years, demonstrating that a

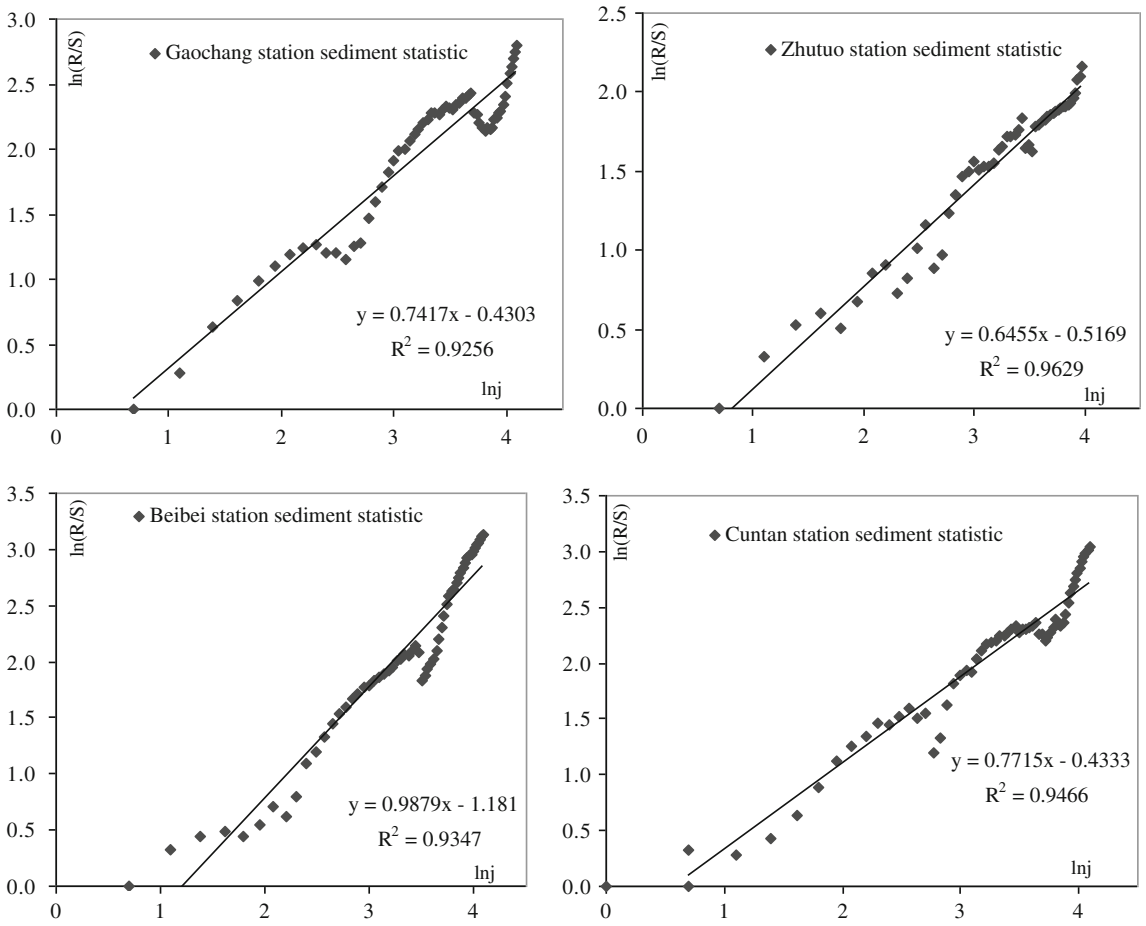

Fig. 6 R/S trend curve of the annual sediment load at the control stations

future annual runoff in the upstream of the Yangtze and Min rivers will maintain a slightly fluctuating pattern, and the Jialing River may maintain an increasing pattern (Fig. 4).

The temporal variation in the sediment load at the control stations from 1954 to 2016 (Fig. 5) showed an overall decline in sediment load at all major stations. There was a reduction in the sediment load at Zhutuo and Beibei stations, and in the main sources of the sediment provided to the Yangtze River, leading to a drastic sediment decrease at Cuntan station as the control point of the TGR, accounting for approximately 53% of the pre-1990 level. As the inflow control point of the upper Yangtze River into the TGR, the UF–UB curve of the annual sediment load at Cuntan station based on the year was used to test the variability of the sediment discharge through the existence of an obvious change in the relationship curve, which began to slightly decrease in 1991 and then leveled off in 2002. These findings indicate a two-stage reduction process of the sediment discharge during the past 60 years: the years 1991 and 2002 can be regarded as the turning point for a reduction of the sediment supply into the TGR. The results

Fig. 7 Relationship between the annual sedimentation and the pool level at the dam

Table 2 Main sedimentation position in the permanent backwater region

No.	Reach section	Channel pattern	Amount of sedimentation ($\times 10^9$ m^3)	Deposition ratio (%)
1	Nearby dam	Broad-valley	1.529	12.1
2	Xiling Gorge	Broad-valley	1.42	11.3
3	Daning River	Broad-valley	0.309	2.5168
4	Chouzi Qi	Broad-valley	0.818	6.5208
5	YunYang	Meander	1.949	15.5584
6	Wanzhou	Meander	0.459	3.6608
7	Zhongzhou	Braided	1.89	15.1008
8	Lanzuba	Braided	1.603	12.8128
9	Fengwei Bar	Braided	0.198	1.6016
10	Yuanyang Pan	Braided	0.209	1.716
Total			10.5	84

were consistent with the previous studies (Zhang and Wen 2004; Xiong et al., 2009; CWRC 2001–2016).

The changing trends of the sediment load at the control stations (Fig. 6) show an H of 0.75, 0.65, 0.98, and 0.8, respectively, at each control point, illustrating that a decreasing trend will occur in the sediment load in the upper Yangtze River, the reduction of the sediment transport in the Jia Lingjiang River will maintain its current level, and Cuntan station will maintain its declining trend.

Spatial variations in the river pattern

In general, a typical reservoir sedimentation process (known as aggradation) continues progressively until a delta forms (Sloff 1991; Fan and Morris 1992). To demonstrate the main deposition reach sections, field measurements for the topography map were collected in the permanent backwater region of the TGR between 2003 and 2013; the entire river channel survey was based on a scale of 1:5000. Unlike in a sand or gravel delta, an alternation of the erosion and accretion processes occurred along the reservoir river reaches (Fig. 7). The sediment deposition in the meandering, broad-valley, and braided reaches of the permanent backwater region reached 10.5×10^9 m^3, accounting for 84% of the total sedimentation (Table 2). The spatial distribution of the main sedimentation along the TGR area (Fig. 7) shows that, in addition to the nearby dam, the river pattern of the reach section is an important control regarding the deposition location in the TGR. In

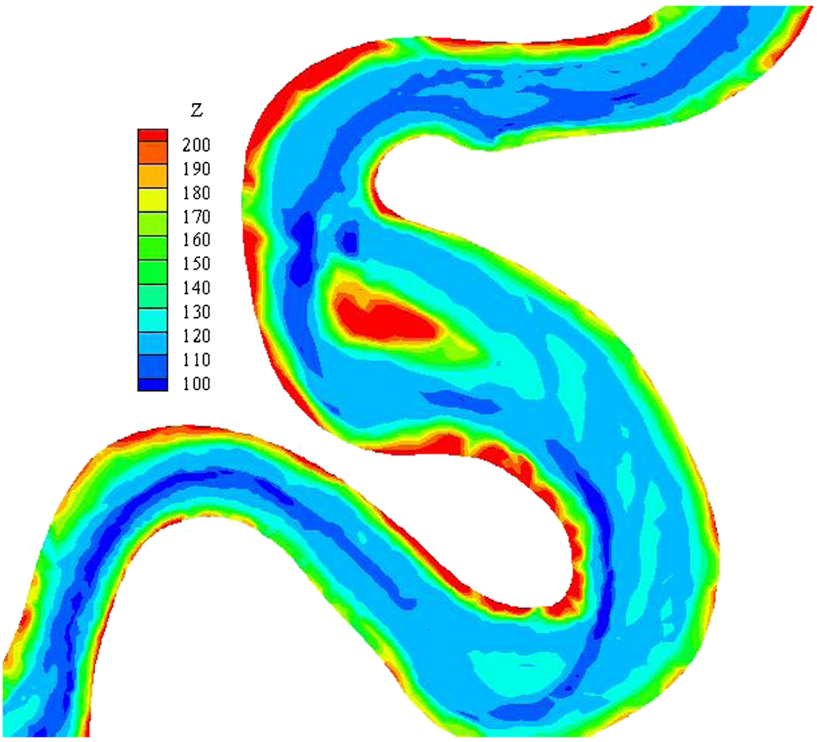

Fig. 8 River bed level of Zhongxian reach in 2012

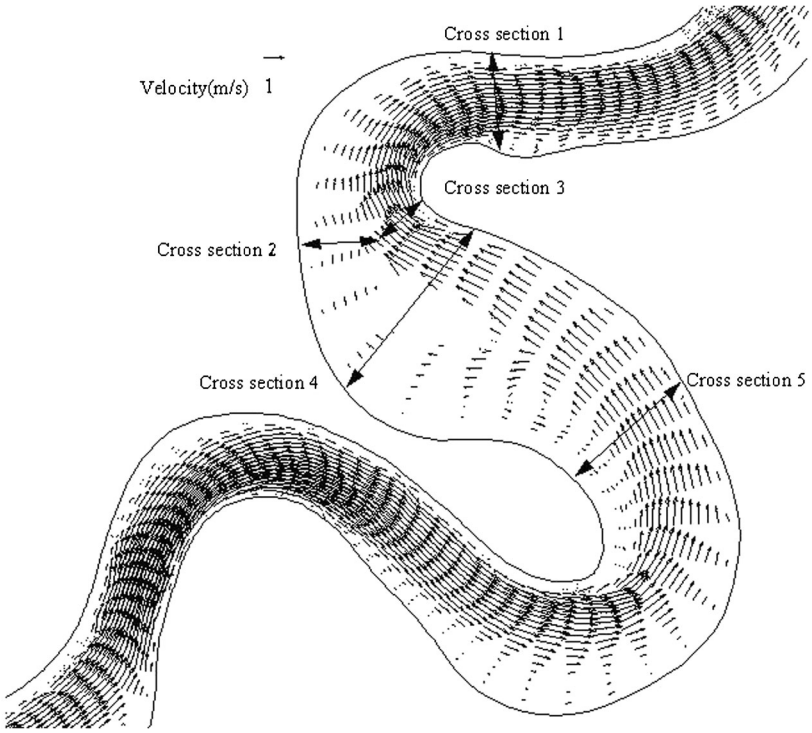

Fig. 9 Flow field in Zhongxian reach

this study, a 2D numerical hydrologic model was applied to simulate the flow field for a typical deposition reach of Zhongxian (Fig. 8) and to analyze the relationship between the channel pattern and location of the deposits.

The 24-km-long study area of the Zhongxian reach is 350 km upstream from the TGR (Fig. 7). The river channel is meandering with a gravel bar exposed during low flows, and the maximum deposition thickness is 52 m, negatively influencing the navigation conditions during the flood period. The peak flood days of June 25, 2012, and June 20, 2013, were selected; the inflow discharge was 63,200 and 44,100 m^3/s, and the water level at the dam was 157.84 and 145.43 m, respectively. Details on the verification of the 2D hydrodynamic numerical model were provided by Xiao et al. (2016).

The contours of the flow velocity in the simulated flow field (Fig. 9) indicate that the velocity in the course on the right of the gravel bar was approximately threefold higher than that on the left. As the flow entered the river bend, the inner bank of the nearby left entrance of the gravel bar had a relatively deep river bed level, leading to a lower velocity compared with the other location of the same cross section (Fig. 10a), which will result in serious sedimentation. The mid-channel bar and the secondary currents contributed to an asymmetrical velocity pattern (Fig. 10b): the velocity of

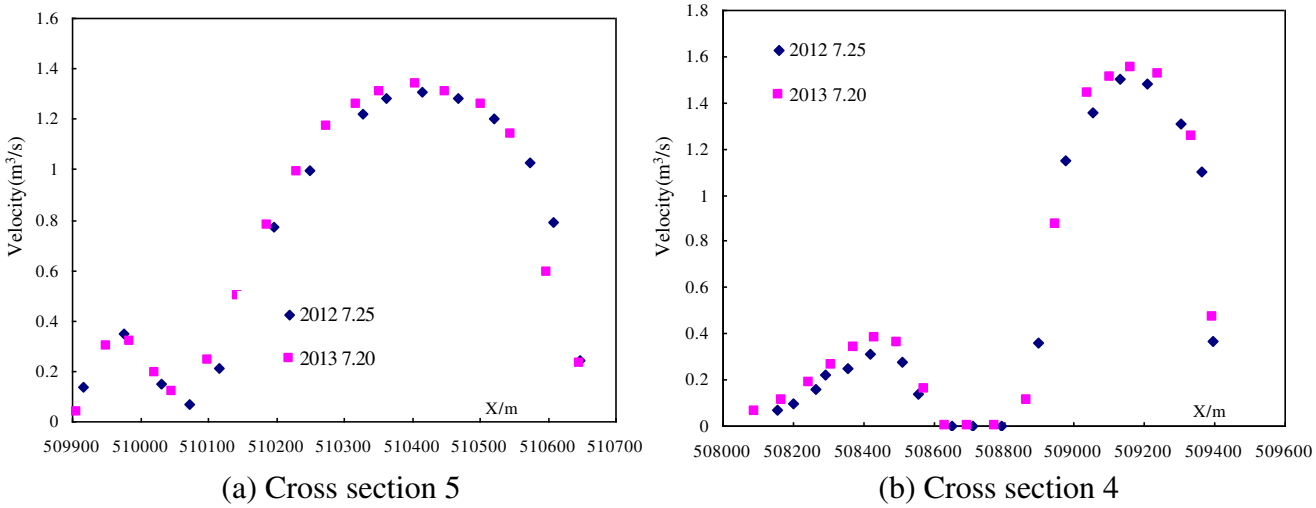

Fig. 10 Velocity profile at the typical cross sections: **a** cross section 5, **b** cross section 4

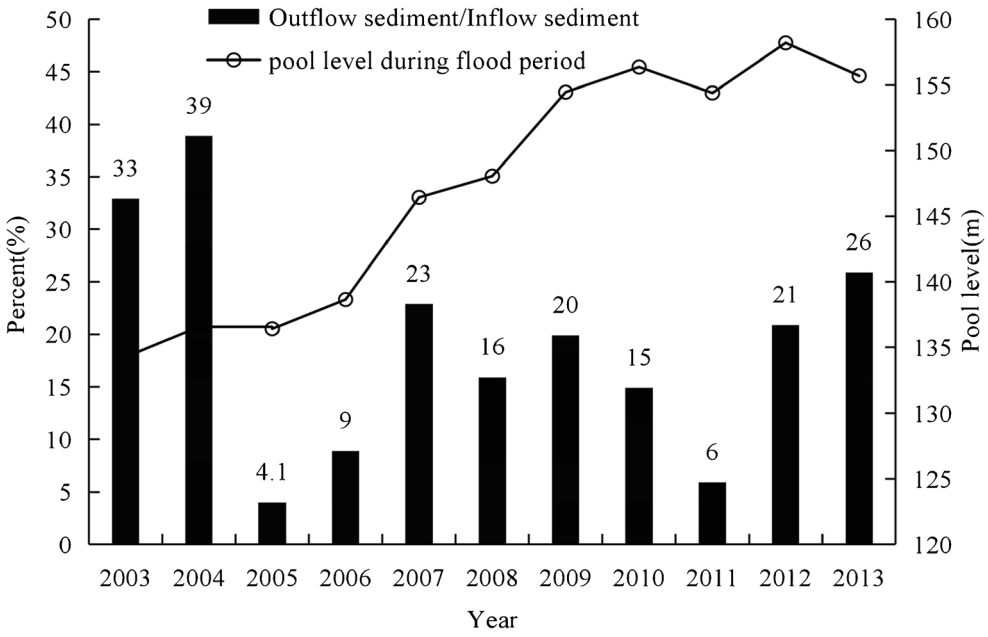

Fig. 11 Main sedimentation reach sections in the Three Gorges Reservoir area

the right course increased to three times that of the left branch, increasing the sediment transport capacity and reducing the deposition. After the flow confluence, the influence of the gravel bar decreased and the velocity recovered to a symmetrical pattern on the tail of the gravel bar. The changing trends of the flow field illustrate the sedimentation in the Zhongxian reach (Fig. 7). This example demonstrates that the river morphology is a controlling factor in the sedimentation process in a river reservoir, particularly a large reservoir with a large backwater region, which directly influences the hydrodynamic conditions and the sediment transport capacity.

Temporal variations in the reservoir operation scheme

The relationship between the annual average pool level at the dam during the flood period and the sediment discharging ratio in the TGR (Fig. 11) shows that the reservoir sedimentation is closely related to the adjustment of the pool level, which controls the hydrodynamic power used to carry the sediment, and that the sedimentation increases with the increase in the pool level during the flood period. Although 2006 and 2011 were dry years with a low sediment transport, most of the inflow sediment was deposited in the reservoir area, and the averaged sediment discharge ratio was only 6% and 9%, corresponding to relatively lower pool levels of 138.7 and 154.4 m, respectively.

Changing trends of the spatial–temporal distribution of sedimentation in the TGR

Based on the analysis of the variable sedimentation process in the TGR, the main controls are the sediment–water discharge relationship, the reservoir operation scheme, and the channel pattern. The pool level at the dam will maintain the 175-145-155 m operation scheme (CWRC 2016), the backwater region

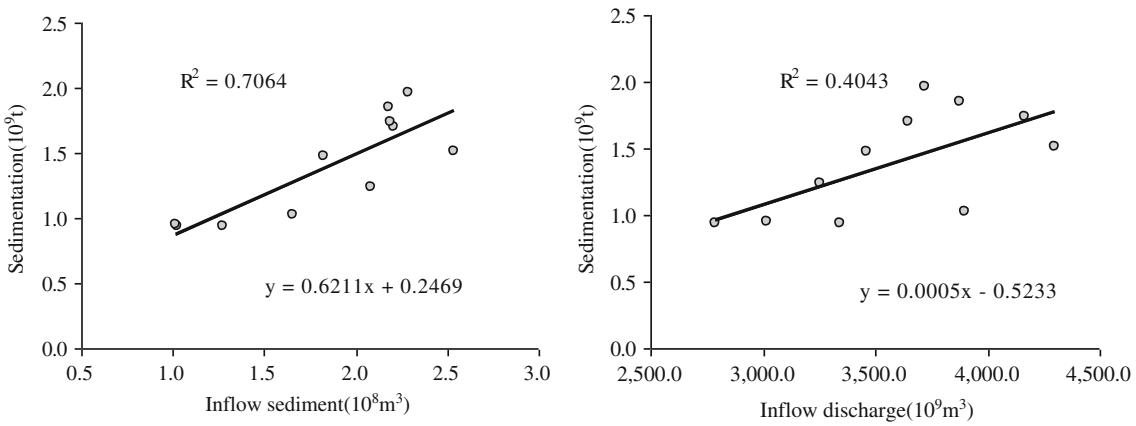

Fig. 12 Relationship between the control factor and reservoir sedimentation

Fig. 13 Dam constructions on the upper Yangtze River

will remain approximately 660 km long in the future, and the changing trends of the main deposition reach sections will maintain the present pattern.

To test the sensitivity of the reservoir sedimentation response to the sediment discharge and the runoff into the TGR, the correlations of the sedimentation–sediment discharge and the sedimentation–runoff relationship were examined (Fig. 12). The regression lines indicate that the sedimentation is more dependent on the sediment discharge (R^2 = 0.7064, which is larger than the value with the runoff change trend of R^2 = 0.4043). Anthropogenic activity has been recognized as the dominant factor in the sharp decrease in sediment load of the Yangtze River in recent years (Xu and Milliman 2009; Wei et al. 2011; Gao et al. 2015). As a result of the reservoir operations on the upper Yangtze River (Jinsha River) and the main tributaries over the following decades (Fig. 13), the sediment discharge will dramatically decrease and lead to a reduction in the sedimentation in the TGR.

Conclusions

The anthropogenic impacts on the channel morphology and fluvial processes include both indirect and direct influences. With the impoundment of the TGR on the upper Yangtze River, the alteration of the hydrodynamic conditions and sediment transport characteristics not only occurs downstream but also in the backwater area of the TGR. After 10 years of operation, the sediment deposited in the TGR reached 1.46 bcm by 2013. Few studies have attempted to determine the main deposition reach sections or the controls for the reservoir sedimentation process. Based on field data from 1954 to 2013, the temporal variation in the relationship of the sediment–runoff shows two turning points for the decreased inflow sediment occurring in 1991 and 2002, illustrating that the inlet condition is not influenced by the operation of the TGR, and that the reduction of the sediment supply will lead to a decreasing trend in the sedimentation process. For the outlet condition, the operation scheme relating to the water level fluctuations in the backwater area directly affects the sedimentation, and the deposition increases with the increase in the pool level at the dam. According to the field measurements of the riverbed map in the backwater area of the TGR, the main deposition reach sections can be classified as meandering, broad-valley, and braided, accounting for approximately 84% of the total sedimentation. The response of the channel pattern to the sedimentation can be a critical factor in controlling the spatial distribution of the deposition. The relationship of the inflow to the discharge–sediment, operation scheme, and channel pattern contributes to the temporal and spatial distribution of the sedimentation in the Three Gorges Reservoir.

Funding information This research is supported by the advanced and applied project of Chongqing Science and Technology (cstc2018jscx-msybX0316).

References

Aleem AA (1972) Effect of river outflow management on marine life. Mar Biol 5:200–208

Batalla RJ, Gomez CM, Kondolf GM (2004) Reservoir-induced hydrological changes in the Ebro River basin(NE Spain). J Hydrol 290: 117–136

Cheng JX, Xu L, Wang XL (2018) Assessment of hydrologic alteration induced by the Three Gorges Dam in Dongting Lake, China. River Res Appl 1:1–11

CWRC (2013) Hydrological data of Changjiang River Basin. Annual hydrological report of P.R. China. Changjiang Water Resources Commission, Beijing ,China

CWRC (2001–2016). Bulletin of Changjiang sediment. Changjiang Press, Wuhan, China

Dai ZJ, Liu JT (2013) Impacts of large dams on downstream fluvial sedimentation: a example of the Three Gorges Dam(TGD) on the Changjiang (Yangtze River). J Hydrol 480:10–18

Dai SB, Lu XX (2014) Sediment load change in the Yangtze River (Changjiang): a review. Geomorphology 215:60–73

Draut AE, Logan JB, Mastin MC (2011) Channel evolution on the dammed Elwha River, Washington, USA. Geomorphology 56: 325–334

Fan J, Morris GL (1992) Reservoir sedimentation, II: Reservoir desiltation and long-term storage capacity. J Hydraul Eng 118: 370–384

Gao P, Wang ZY, Donald S (2015) Spatial and temporal sedimentation changes in the Three Gorges Reservoir of China. Lakes Reserv Res Manag 20:232–242

Graf WL (2006) Downstream hydrologic and geomorphic effects of large dams on American rivers. Geomorphology 79:336–360

Guo H, Qi H, Zhang Q, Feng S (2012) Effects of the Three Gorges Dam on Yangtze River flow and river interaction with Poyang lake, China:2003-2008. J Hydrol 416:19–27

Kiss T, Fiala K, Sipos G (2008) Alterations of channel parameters in response to river regulation works since 1840 on the lower Tisza River(Hungary). Geomorphology 98:96–110

Kummu M, Lu XX, Wang JJ, Varis O (2010) Basin-wide sediment trapping efficiency of emerging reservoirs along the Mekong. Geomorphology 119:181–187

Li QF, Yu MX, Lu GB, Cai T (2011) Impacts of the Gezhouba and Three Gorges reservoirs on the sediment regime in the Yangtze River, China. J Hydrol 403:224–233

Lien HC, Hsieh TY, Yang JC, Yeh KC (1999) Bend flow simulation using 2D depth- averaged model. J Hydraul Eng 125(10):1097–1108

Lu X, Jiang T (2009) Larger Asian rivers: climate change, river flow and sediment flux. Quat Int 208:1–3

Marwan AH, Church M, Yan XL, Slaymaker O (2011) Suspended sediment balance for the mainstem of Changjiang (Yangtze River) in the period 1964-1985. Hydrol Process 25:2339–2353

Nilsson C, Reidy CA, Dynesius M, Revenga C (2005) Fragmentation and flow regulation of the world's large river systems. Science 308:405–408

Sediment-Panel (2016) Study on sediment problems in the Three Gorges Project on the Yangtze River (in Chinese). Construction committee for the Three Gorges Project. State Council of China, Beijing

Sloff CJ (1991) Reservoir sedimentation in reservoirs: literature review, Report No. 91-2, Civil Engineering Department. Delft University of Technology, Delft

Sneyers R(1990) On the statistical analysis of series of observations. Tech Note 143, WMO-No 415 192

Sun ZD, Huang Q, Opp C, Henning T, Marold U (2012) Impacts and implications of major changes caused by the Three Gorges Dam in the middle reaches of the Yangtze River, China. Water Resour Manag 26:3367–3378

Wang SJ, Yan YX, Li YX (2012) Spatial and temporal variations of suspended sediment deposition in the alluvial reach of the upper Yellow River from 1952 to 2007. Catena 92:30–37

Wei J, He X, Bao Y (2011) Anthropogenic impacts on suspended sediment load in the Upper Yangtze river. Reg Environ Chang 11:857–868

Wolf A, Bergmann A, Wilken RD, Gao X (2013) Occurrence and distribution of organic trace substances in waters from the Three Gorges Reservoir, China. Environ Sci Pollut Res 20:7124–7139

Xiao Y, Shao XJ, Wang H, Zhou G (2012) Formation process of meandering channel by a 2D numerical simulation. Int J Sediment Res 3:306–322

Xiao Y, Zhou G, Yang SF (2016) 2D numerical modelling of meandering channel formation. J Earth Syst 2(125):251–267

Xiong M, Xu QX, Yuan J (2009) Analysis of multi-factors affecting sediment load in the Three Gorges Reservoir. Quat Int 208:76–84

Xu KH, Milliman JD (2009) Seasonal variations of sediment discharge from the Yangtze River before and after impoundment of the Three Gorges Dam. Geomorphology 104:276–283

Yan QY, Yu YH, Feng WS (2008) Plankton community composition in the Three Gorges Reservoir Region revealed by PCR-DGGE and its relationships with environmental factors. J Environ Sci 20:732–738

Yang ZJ, Liu DF, Ji DB, Xiao SB (2010) Influence of the impounding process of the Three Gorges Reservoir up to water level 172.5 m on water eutrophication in the Xiangxi Bay. Sci China Technol Sci 53: 1114–1125

Yang SL, Milliman JD, Li P, Xu K (2011) 50,000 dams later: erosion of the Yangtze River and its delta. Glob Planet Chang 75:14–20

Yue S, Pilon P, Phinney B, Cavadias G (2002) The influence of autocorrelation on the ability to detect trend in hydrological series. Hydrol Process 16:1807–1829

Zhang XB, Wen AB (2004) Current changes of sediment yields in the upper Yangtze River and its two biggest tributaries, China. Glob Planet Chang 41:221–227

Zhang JX, Liu ZJ, Sun XX (2009) Changing landscape in the Three Gorges Reservoir Area of Yangtze River from 1977 to 2005: land use/land cover, vegetation cover changes estimated using multi-source satellite data. Int J Earth Observ 11:403–412

Zhou P, Zhuang WH, Wen AB (2016) Fractal features of soil particle redistribution along sloping landscapes with hedge berm in the Three Gorges Reservoir Region of China. Soil Use Manag 32: 594–602